

# Depth of focus increase by multiplexing programmable diffractive lenses

C. Iemmi

*Departamento de Física, Facultad de Ciencias Exactas y Naturales, Universidad de Buenos Aires, 1428 Buenos Aires, Argentina.*  
[iemmi@df.uba.ar](mailto:iemmi@df.uba.ar)

J. Campos, J. C. Escalera, O. López-Coronado, R. Gimeno and M. J. Yzuel

*Departamento de Física, Universidad Autónoma de Barcelona, 08193 Bellaterra, Spain.*  
[Juan.Campos@uab.es](mailto:Juan.Campos@uab.es)

**Abstract:** A combination of several diffractive lenses written onto a single programmable liquid crystal display (LCD) is proposed for increasing the Depth of Focus (DOF) of the imaging system as a whole. The lenses are spatially multiplexed in a random scheme onto the LCD. The axial irradiance distribution produced by each lens overlaps with the next one producing an extended focal depth. To compare the image quality of the multiplexed lenses, the Modulation Transfer Function (MTF) is calculated. Finally we obtain the experimental Point Spread Functions (PSF) for these multiplexed lenses and experimental results in which an extended object is illuminated under spatially incoherent monochromatic light. We compare the images obtained in the focal plane and in some defocused planes with the single lens and with three multiplexed lenses. The experimental results confirm that the multiplexed lenses produce a high increase in the depth of focus.

©2006 Optical Society of America

**OCIS codes:** (50.1970) Diffractive optics; (230.3720) Liquid-crystal devices; (230.6120) Spatial Light Modulators; (220.3620) Lens design.

---

## References and links

1. H. Fukuda, "A new pupil filter for annular illumination in optical lithography," *Jpn. J. Appl. Phys.* **31**, 4126-4130 (1992).
2. R. Hild, M. J. Yzuel and J. C. Escalera, "High focal depth imaging of small structures," *Microelectron. Eng.* **34**, 195-214 (1997).
3. G. G. Yang, "An optical pickup using a diffractive optical element for a high-density optical disc," *Opt. Commun.* **159**, 19-22 (1999).
4. H. Wang and F. Gan, "High focal depth with a pure-phase apodizer," *Appl. Opt.* **40**, 5658-5662 (2001).
5. W. T. Welford, "Use of annular aperture to increase focal depth," *J. Opt. Soc. Am. A* **50**, 749-753 (1960).
6. Z. S. Hegedus, "Annular pupil arrays. Application to confocal scanning," *Opt. Acta.* **32**, 815-826 (1985).
7. J. C. Escalera, M. J. Yzuel and J. Campos, "Control of the polychromatic response of an optical system through the use of annular color filters," *Appl. Opt.* **34**, 1655-1663 (1995).
8. C. J. R. Sheppard and Z. S. Hegedus, "Axial behaviour of pupil-plane filters," *J. Opt. Soc. Am. A* **5**, 643-647 (1988).
9. C. S. Chung and H. H. Hopkins, "Influence of non-uniform amplitude on PSF," *J. Mod. Opt.* **35**, 1485-1511 (1988).
10. J. Ojeda-Castañeda, E. Tepichin and A. Díaz, "Arbitrarily high focal depth with quasioptimum real and positive transmittance apodizer," *Appl. Opt.* **28**, 2666-2670 (1989).
11. J. Ojeda-Castañeda, L. R. Berriel Valdos and E. Montes, "Spatial filter for increasing the depth of focus" *Opt. Lett.* **10**, 520-522 (1985).
12. M. J. Yzuel, J. C. Escalera and J. Campos, "Polychromatic axial behavior of axial apodizing and hyperresolving filters," *Appl. Opt.* **29**, 1631-1641 (1990).

13. J. Ojeda-Castañeda and L. R. Berriel-Valdos, "Zone plate for arbitrarily high focal depth," *Appl. Opt.* **29**, 994-996 (1990).
  14. G. Indebetow and H. Bai, "Imaging with Fresnel zone pupil masks: extended depth of field," *Appl. Opt.* **23**, 4299-4302 (1984).
  15. J. Davis, J. C. Escalera, J. Campos, A. Márquez, M. J. Yzuel and C. Iemmi, "Programmable axial apodizing and hypersolving amplitude filters with a liquid-crystal spatial light modulator" *Opt. Lett.* **24**, 628-630 (1999).
  16. A. Márquez, C. Iemmi, J. Campos, J. C. Escalera, and M. J. Yzuel, "Programmable apodizer to compensate chromatic aberration effects using a liquid crystal spatial light modulator," *Opt. Express* **13**, 716-730 (2005).
  17. A. Márquez, C. Iemmi, J. C. Escalera, J. Campos, S. Ledesma, J. Davis and M. J. Yzuel, "Amplitude apodizers encoded onto Fresnel lenses implemented on a phase-only spatial light modulator" *Appl. Opt.* **40**, 2316-2322 (2001).
  18. T. R. M Sales and G. M. Morris, "Diffractive superresolution elements," *J. Opt. Soc. Am. A* **14**, 1637-1646 (1997).
  19. S. Ledesma, J. C. Escalera, J. Campos, and M. J. Yzuel, "Evolution of the transverse response of an optical system with complex filters," *Opt. Commun.* **249**, 183-192 (2005).
  20. W. T Cathey, E. R. Dowski, "New paradigm for imaging systems," *Appl. Opt.* **41**, 5658-5662 (2001).
  21. E. Ben-Eliezer, Z. Zalevsky, E. Marom and N. Konforti, "All-optical extended depth of field imaging system," *J. Opt. A: Pure Appl. Opt.* **5**, S164-S169 (2003).
  22. A. Márquez, C. Iemmi, J. Campos, and M. J. Yzuel, "Achromatic diffractive lens written onto a liquid crystal display," *Opt. Lett.* **31**, 392-394 (2006).
  23. A. Márquez, C. Iemmi, I. Moreno, J. A. Davis, J. Campos and M. J. Yzuel, "Quantitative prediction of the modulation behavior of twisted nematic liquid crystal displays based on a simple physical model," *Opt. Eng.* **40**, 2558-2564 (2001).
- 

## 1. Introduction

Many optical systems need a long Depth of Focus (DOF). For instance, in optical microlithography high DOF is needed to obtain a stable image in the photoresist [1, 2]. High density optical data storage requires high-numerical aperture (NA) lenses and short wavelengths. But increasing NA and decreasing wavelength, the DOF decreases rapidly. So, different techniques are used to improve the axial response [3-4].

Different optical methods have been used to increase the depth of focus. Annular pupils produce an increase both of the DOF and the resolution [5-7] at the expense of an increase in sidelobes and loss of light. Non-uniform transmission filters have been also proposed to increase DOF [8-11], also with polychromatic illumination [12]. In that line, a zone plate with a prespecified number of foci [13], which are separated axially by Rayleigh's limit of resolution was proposed to create arbitrarily high DOF. Fresnel zone pupil masks have been also used [14]. It was demonstrated that amplitude-transmitting filters for apodizing and hyperresolving applications can be implemented with a two-dimensional programmable liquid-crystal spatial light modulator (LCSLM) operating in an amplitude-only mode [15,16] or they can be encoded onto Fresnel lenses on a phase-only SLM [17]. In all these cases, the loss of light is the main drawback.

In an effort to improve light throughput efficiency, different works have studied phase only filters. In some cases, the main goal is to obtain transverse superresolution [18]. The possibility of improving DOF using phase only filters has also been investigated [4]. The transverse response at defocused planes produced by complex filters with high focal depth was studied in [19]. Cathey et al [20] proposed a two step procedure: first a phase element apparently degrades the image, but a digital post-processing treatment improves the DOF. In methods like this, it is important that there is no loss of spatial frequencies in the first step in order to recover later all the image information. The increase of the DOF was obtained in [21] in a one step all-optical system, consisting of a lens plus a non-absorptive composite phase mask (CPM), consisting of several spatially multiplexed Fresnel lenses. In this paper only simulated results were presented. In other cases the phase element is produced in a liquid crystal spatial light modulator. For instance, in [22] it was proposed a programmable diffractive lens written onto a liquid crystal display that is able to provide equal focal lengths

for several wavelengths simultaneously. An appropriate lens for each wavelength was designed, and these lenses were spatially multiplexed onto the LCD.

In this paper we propose a combination of several diffractive lenses written onto a single programmable LCD. The lenses are spatially multiplexed in a random scheme onto the LCD. The axial irradiance distribution produced by each lens overlaps with the next one producing an extended focal depth. The global effect is an increase in the DOF. In section 2 we describe the technique used to multiplex the lenses. We also study the Modulation Transfer Function (MTF) produced by the single lens and the different multiplexed lenses, in order to compare the image quality. In section 3 we show experimental results of the Point Spread Function (PSF) and also of different tests with extended objects for the single lens and the multiplexed lenses. These results confirm the feasibility of multiplexing lenses to increase the DOF.

## 2. Multiplexed lenses

### 2.1 Lenses design

As we previously mentioned the aim of this work is to propose a method to increase the depth of focus of a diffractive lens. It is well known that by means of programmable spatial light modulators it is possible to control pixel by pixel the phase distribution of a wave front [23]. Taking profit of this feature we propose a combination of several diffractive lenses written onto a single programmable liquid crystal display (LCD). Each lens is designed in such a way that lenses with consecutive focal lengths provide amplitude distributions along the axis that overlap. These lenses are spatially multiplexed. In a previous paper [22] we have shown that among the different multiplexing possibilities, random multiplexing give place to a system whose point spread function has reduced transversal sidelobes so, it is adequate to image extended objects.

Our LCD has VGA resolution (640 X 480 pixels) with a pixel width of 34  $\mu\text{m}$  and a pixel distance (from the center of one pixel to the center of the next one) of 41  $\mu\text{m}$ , then the generated lenses have a 480 pixels diameter which is equivalent to 19.68 mm. The sampling of a Fresnel lens causes the appearance of multiple lenses when the sampling frequency is lower than the Nyquist frequency. To avoid this effect we design lenses with a focal length of about 100 cm for the blue line of an Ar laser ( $\lambda = 458 \text{ nm}$ ).

In the random multiplexing technique the aperture is divided in sub apertures of  $P \times P$  pixels, each sub aperture will be randomly assigned to a different lens, and then the transmission of the pixels of this sub aperture is taken from the corresponding lens.

The random assignment is performed as follows. For each sub aperture of the pupil a random number  $k$  in the range  $(0, N]$  is generated. Let the number  $k$  fall in the range  $j-1 < k \leq j$  with  $j$  an integer number. Then the phase values of the sub aperture pixels are taken from the lens  $j$ . In Fig. 1 we show a diagram of this technique for building a multiplexed lens with  $3 \times 3$  pixels sub apertures.

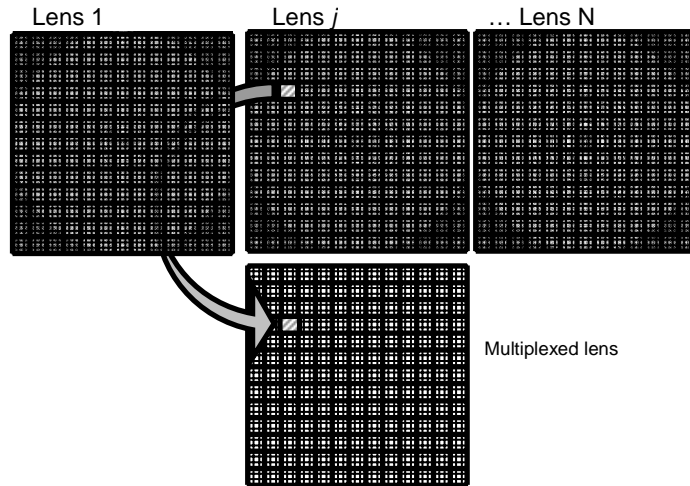


Fig. 1. Random multiplexing scheme. For each sub aperture a lens is chosen randomly and the transmission of its pixels assigned to the multiplexed lens.

In this work we have chosen sub apertures of  $1 \times 1$  pixel size to build three multiplexed lenses that cover a focal range from 92 cm to 108 cm, the first one (see Fig 2-b) resultant of multiplexing 9 lenses, the interval between consecutive focal lengths being 2 cm; a lens resultant of multiplexing 17 lenses, with 1 cm between consecutive focal lengths; and a lens resultant of multiplexing 33 lenses [see Fig. 2(c)] with a spacing of 0.5 cm between consecutive focal lengths.

In Figs. 2 (a)-2(c) we show a single lens (hereafter SL) with a focal length of 100 cm, a lens resultant of multiplexing 9 lenses (hereafter M9) with focal lengths ranging from 92 cm to 108 cm, i.e. the interval between consecutive focal lengths is 2 cm, and a lens resultant of multiplexing 33 lenses (hereafter M33) with focal lengths ranging from 92 cm to 108 cm, i.e. now the interval between consecutive focal lengths is 0.5 cm. This focal depth range has been chosen arbitrarily. Once we have chosen this focal range, we search for multiplexed lenses that produce an axial response as good as possible. We will show that we can implement a multiplexed lens with a number of lenses enough to produce a smooth (almost constant) axial response.

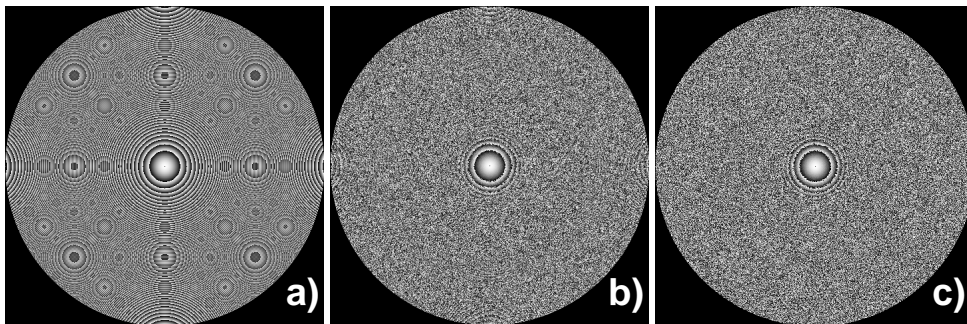


Fig. 2. (a) a single diffractive lens, (b) 9 lenses multiplexed and (c) 33 lenses multiplexed.

In principle the multiplexed lenses must produce focalizations at different planes since each of the constitutive lenses will focus in a different location. In order to study the effect of the random pupil and the defocused light on the final image, in the next subsection we will analyze the transfer function of these three diffractive elements.

## 2.2 Modulation Transfer Function of the multiplexed lenses

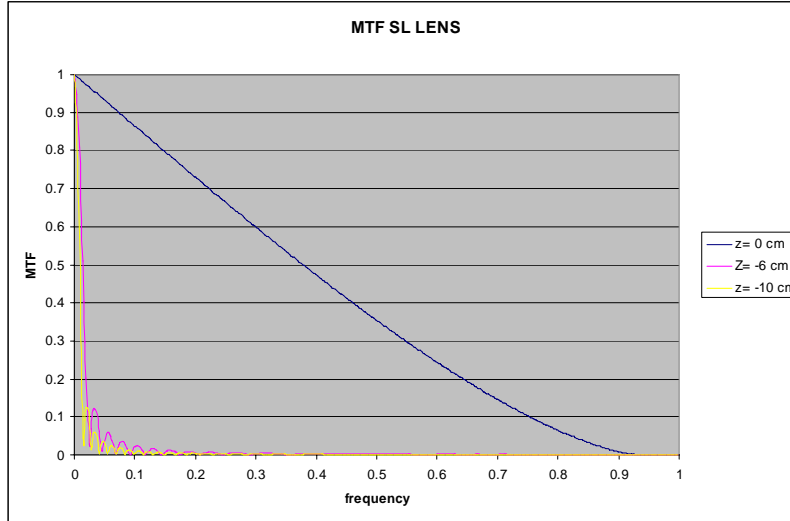


Fig. 3. MTF of the single lens in three planes

In order to compare the image quality of the SL lens with the M9 and M33 multiplexed lenses, we have calculated the Modulation Transfer Function (MTF) in the three cases. We have calculated the MTF in three planes, in the Best Image Plane (BIP,  $Z=0$  cm) and in two arbitrary chosen defocused planes:  $Z=-6$  cm and  $Z=-10$  cm, (6 cm and 10 cm closer to the LCD respectively).

The MTF for a given multiplexed lens and for a focusing plane at a distance  $d$  from the lens is evaluated as follows. Let  $L(x,y) = \exp[i\phi(x,y)]$  be the phase transmission of the multiplexed lens. This matrix with an original size of  $480 \times 480$  pixels is zero padded to a size of  $1024 \times 1024$  pixels (it should have at least double size than the original and take a power of 2). This transmission is multiplied by the phase corresponding to the Fresnel propagation a distance  $d$ :  $F(x,y) = \exp[-(i\pi/\lambda d)(x^2 + y^2)]$ . The result is Fourier transformed. The modulus square of the result is the Point Spread Function (PSF) at a distance  $d$  from the lens. With a second Fourier transform the Optical Transfer Function (OTF) is obtained. In Figs. 3-6 section of the modulus of the OTF (MTF) are plotted. For the random multiplexed lenses only one realization (the one used in the experiments) is evaluated and for this reason, there are random fluctuations in the MTF (see Figs. 5 and 6).

Figure 3 shows the MTF produced by the SL lens. We can see a very good response in the  $Z=0$  cm plane that is deteriorated strongly in the defocused planes.

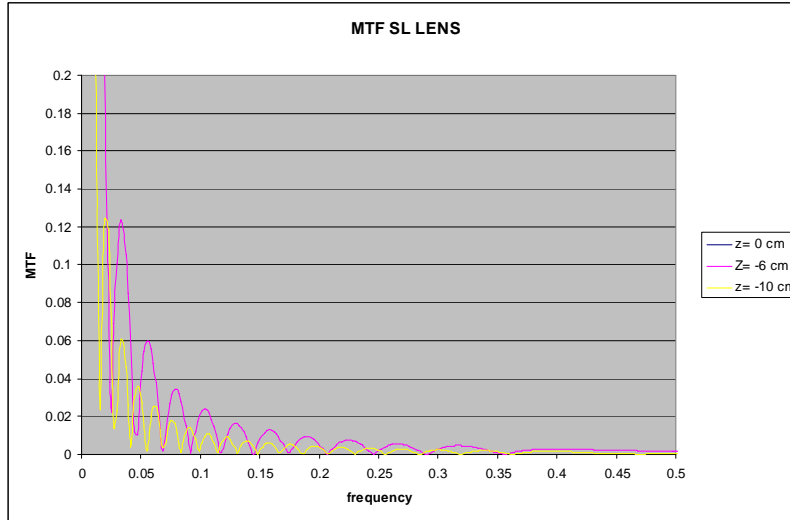


Fig. 4. MTF of the single lens in three planes (zoom of the region of interest)

Figure 4 shows a zoom of a region of interest in Fig. 3. We can see that in these range of spatial frequency there are a lot of contrast inversions. Each time that the MTF value is equal to 0, then a contrast inversion is produced. The image information that corresponds to those frequencies is lost, even if a post-processing is done. So, we expect a bad image quality in these defocused planes.

Figures 5 and 6 show the MTF produced by the M9 and M33 lenses respectively in the BIP ( $Z=0$ ) and in two defocused planes. If we compare Figs. 5 and 6 with Fig. 4 we see that the MTF in the BIP is obviously better for the SL. Both M9 and M33 lenses produce a strong descend in the MTF except for frequency 0. We expect a high background noise superposed to the object image. That can be appreciated in the experimental results shown in section 3. This background noise can be easily removed by subtracting a constant value to the whole image. This is the main drawback of the multiplexed lens, and a high dynamic range camera should be needed to capture correctly the image.

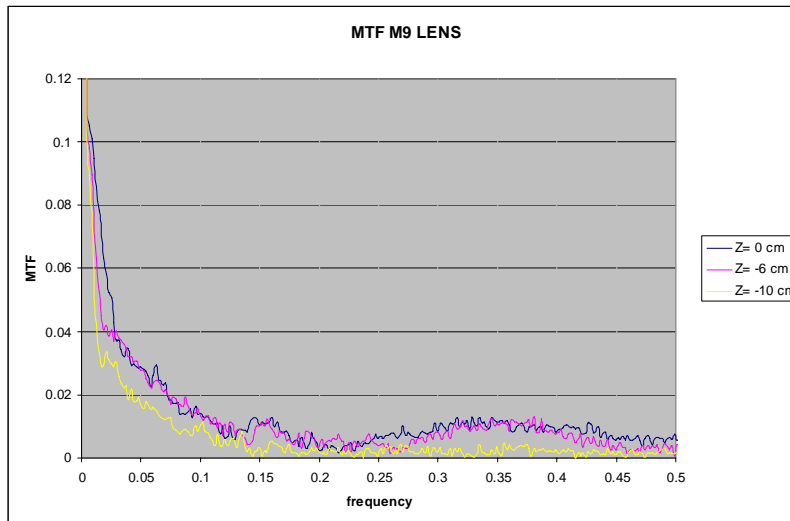


Fig. 5. MTF of the nine multiplexed lens in three planes

But an advantage is that both the M9 and M33 lenses produce a far better response in the defocused planes. The M9 (Fig. 5) lens does not produce contrast inversions in the [0-0.1] frequency region (the SL lens produces at least 4 contrast inversion in that region, see Fig. 4). Nevertheless, one contrast inversion is appreciated in the [0.1-0.2] frequency region and another in the [0.2-0.45] frequency regions for  $Z=0$  cm and  $Z=-6$  cm. The MTF of the M33 lens in the defocused planes is even better and there is a smooth decay with no trace of contrast inversions in the whole [0-0.5] frequency region. So, we expect an image improvement in the defocused planes, especially with the M33 lens with respect to the SL lens. This behaviour is experimentally studied in the next section.

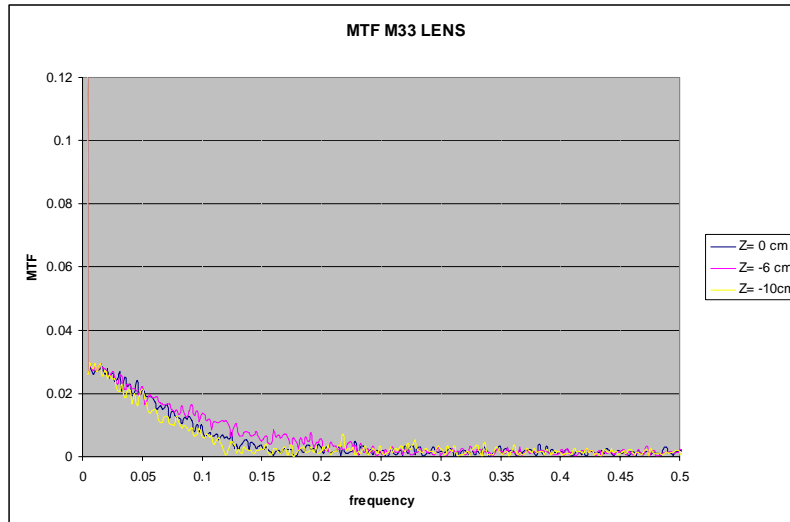


Fig. 6. MTF of the 33 multiplexed lens in three planes

### 3. Experimental results

#### 3.1 Optical set-up

A scheme of the experimental setup for imaging extended objects is shown in Fig. 7. The blue line of an  $\text{Ar}^+$  laser ( $\lambda = 458$  nm) is used as light source. The laser beam impinges onto a ground glass rotating diffuser D and the object O is uniformly illuminated by means of the condenser C. The object is placed in the focus plane of lens L, in this way it is imaged in the focal plane of the diffractive lens shown in the liquid crystal display LCD. The system composed by polarizer P1 and wave plate WP1 constitutes a polarization state generator, analogously the system composed by WP2 and P2 constitutes a polarization state detector. These sets together with the LCD conform a spatial light modulator. By following the optimization procedure proposed in [23] it is possible to obtain a configuration of polarization states that provides phase only modulation. In this work we use a Sony liquid crystal panel, model LCX012BL, extracted from a Sony videoprojector model VPL-V500. The phase shift dynamic range is close to  $360^\circ$  at 458 nm and the amplitude modulation is almost flat. For capturing the Point Spread Function (PSF), a spatial filter is situated between the laser and lens L. The diffuser D and the condenser C are withdrawn. The spatial filter produces the point source that is placed in the focus of lens L.

The images of the extended object and the PSF are captured by a cooled digital 14 bit CCD camera, model PCO.2000 with 2048x2048 pixels,  $7.4 \times 7.4 \mu\text{m}^2$  pixel size. As we will see later, a high dynamic range camera is needed because some of the images contain a high background. With an 8 bit CCD camera this background would fill all the dynamic range of the camera and images with very low quality would be obtained.

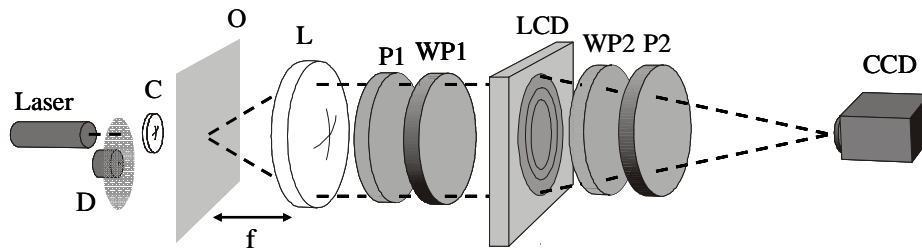


Fig. 7. Scheme of the imaging set-up for extended objects. D is a rotating diffuser, C a condenser, O is the object placed in the focal plane of lens L. P1 and P2 are polarizers, WP1 and WP2 are wave plates that together with the liquid crystal display LCD conform the pure phase modulator used to display the diffractive lenses. An image of O is captured by a CCD camera.

In order to compare experimentally the responses of the diffractive elements described in Section 2 we displayed the lenses onto the LCD and by shifting the CCD camera along the axis we registered the PSF of the system and the images of the extended object O at different planes in different experiments.

### 3.2 Point Spread Function of the multiplexed lenses

We have experimentally obtained the PSF of the SL, the M9 and the M33 multiplexed lenses, and of an additional intermediate multiplexed lens formed by 17 lenses (hereafter M17) with focal lengths ranging from 92 cm to 108 cm, with an interval of 1 cm between consecutive focal lengths, also designed as explained in section 2.1.

For each lens, we captured images of the point source along the optical axis and measured the intensity at the center of each image. It is shown in Fig. 8 the intensity profile along the axis for each lens. The axial intensity distributions produced by the SL lens and the M9, M17 and M33 lenses are shown in Fig. 8(a). In Fig. 8(b) we show in a different scale the intensity distributions produced by the M9, M17 and M33 lenses. It can be seen that M33 has the most smooth and constant profile through the axis, while maintaining a good DOF. On the contrary, in M17 and M9 the intensity shows more variations due to the increase on the distance between the different focuses. We can estimate the DOF looking for the Full Width at Half Maximum (FWHM) in Fig. 8(a). Figure 8(a) shows that the FWHM for the single lens is about 10 mm. Figure 8(b) shows that the FWHM for the M33 is about 200 mm. It is important to note that only the M33 lens produces a sufficient uniform axial response to consider that the DOF has been enhanced. This study suggests that the M33 is the best solution to obtain a high focal depth in the chosen axial region.



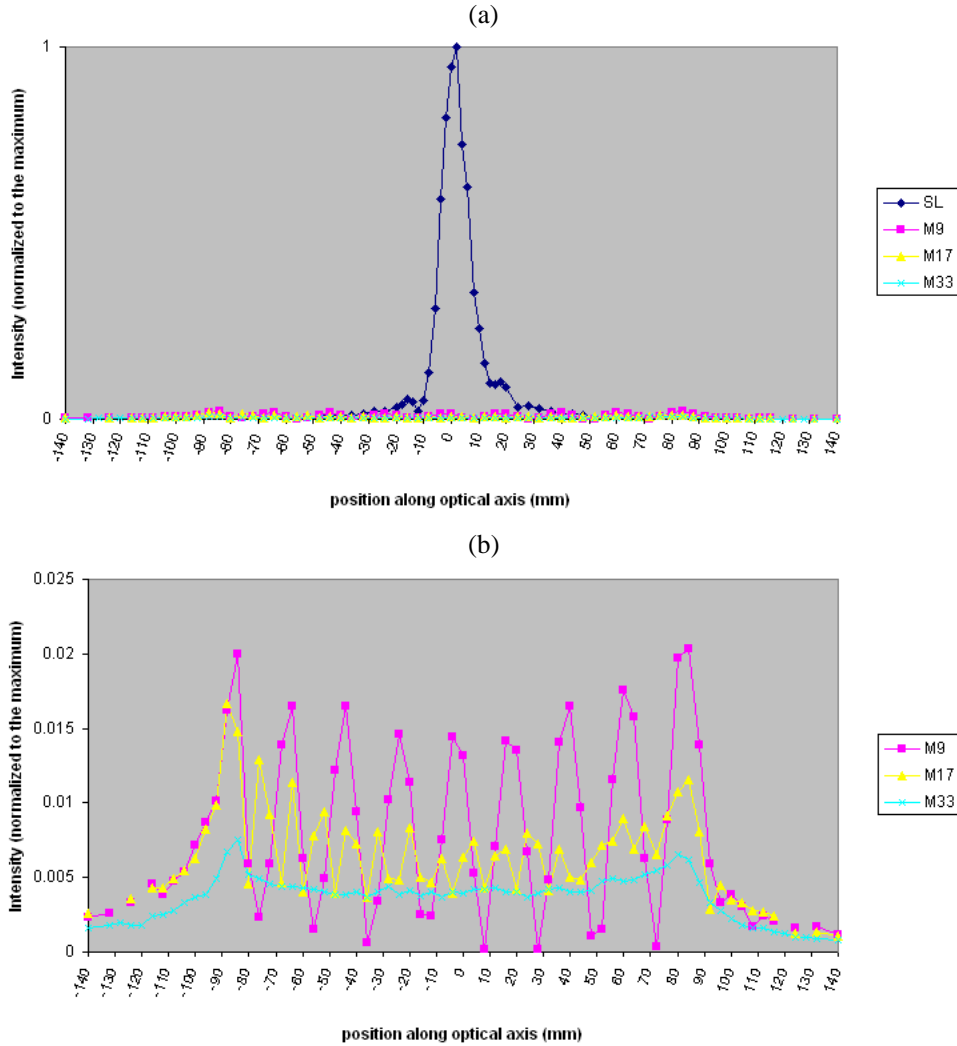


Fig. 8. Intensity profile of the PSF along the axis for SL, M9, M17 and M33 lenses (a); and for just M9, M17 and M33 lenses (b). Position  $Z=0$  corresponds to Best Image Plane (BIP)

Figure 9 shows experimental PSF at  $Z=0$  (BIP),  $Z=-6$  cm and  $Z=-10$  cm for each lens. The principal maximum of the PSF in the BIP for the M9, M17 and M33 lenses is wider than for the SL. This fact suggests that it will be a decrease of resolution in the BIP with the multiplexed lenses. The PSF in the planes  $Z=-6$  cm and  $Z=-10$  cm produced by the SL is almost null. On the contrary, the multiplexed lenses maintain a much better response in those planes.

It can be seen that M33 performs the most constant PSF along the axis, though resulting in a quite wide spot. On the other side, M9 performs alternatively focused and defocused PSFs, with M17 having an intermediate behavior.

If we compare the PSF in the BIP produced by the M9 and M33 lenses, we see that the M33 produces a more uniform PSF. The M9 produces a strong annular sidelobe that will deteriorate the image in the BIP. We will confirm this comparison with the study of the extended object images in the next section.

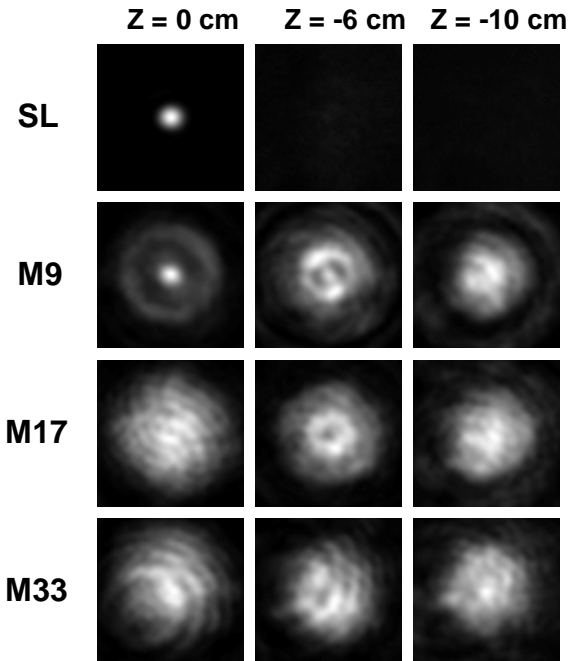


Fig. 9. PSF of the simple and multiplexed lenses, captured at three different planes.

### 3.3 Extended object images

We use in this experiment two types of objects: a Siemens star and a resolution target. In order to compare the responses of lenses with a different amount of multiplexed lenses we captured images of the Siemens star and the resolution target at  $Z = 0$  with the M9 and the M33 lenses. The results are summarized in Fig. 10.

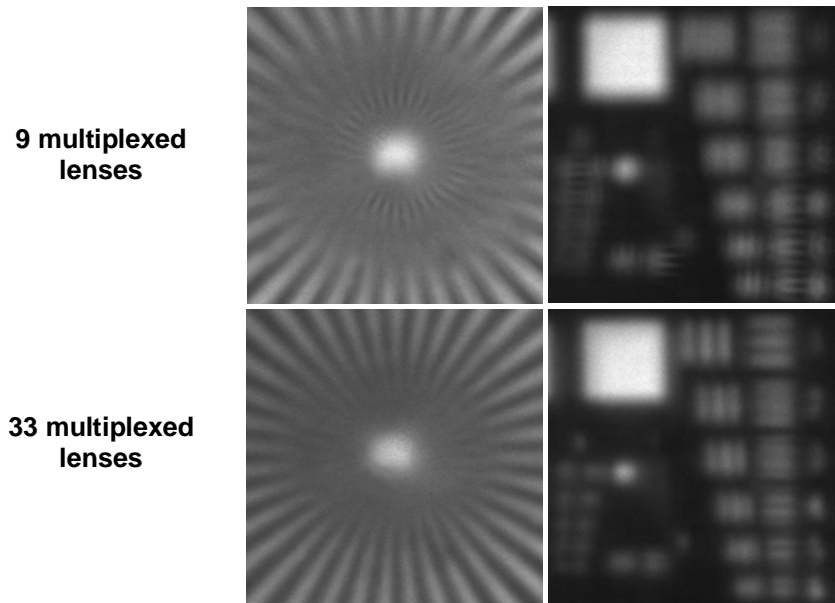


Fig. 10. Images of an enlarged portion of the Siemens star and the resolution test captured at  $Z = 0$  plane when 9 multiplexed lenses and 33 multiplexed lenses are used

It is noticeable from Fig. 10 that some contrast inversions are evident for the M9 lens and zero values for the MTF appear in this case. We can also observe that the M33 lens does not produce contrast inversions in those frequency regions. So, we conclude that the M33 produces a better response in the BIP. These results are in agreement with the MTF's shown in Figs. 5 and 6 and with the PSF's shown in Fig. 9.

Images of the Siemens star are shown in Fig. 11. They are obtained by using the single lens and the multiplexed 33 lenses. The best image plane (BIP) for the single lens is placed at 100 cm from the LCD, we will identify this plane with  $Z=0$ . We also show how the defocus degrades the image as the CCD is farther from that plane. Images were captured when the defocus is of -6 cm and -10 cm. When the multiplexed lens is used the images maintain their quality in the entire range of distances.

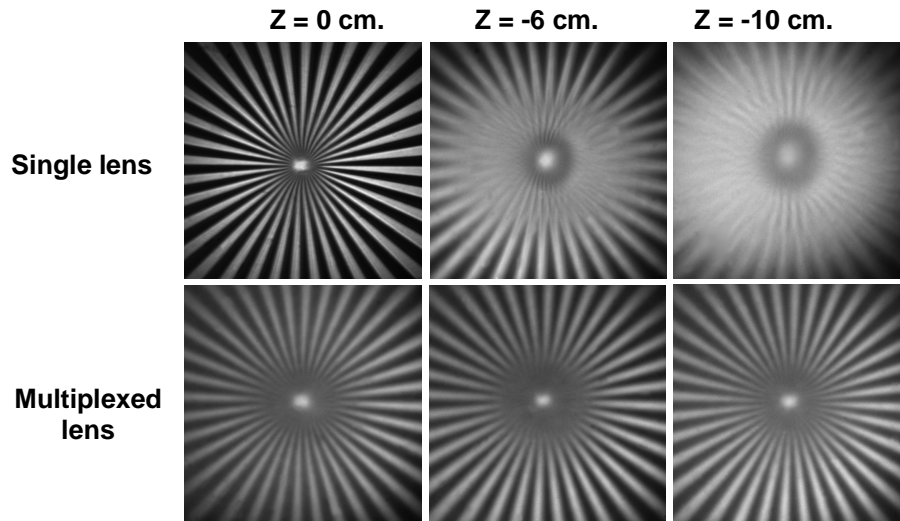


Fig. 11. Images of the Siemens star captured at the best image plane ( $Z = 0$ ) and defocused planes ( $Z = -6$  cm and  $Z = -10$  cm) when a single lens and a multiplexed lens (M33) are used.

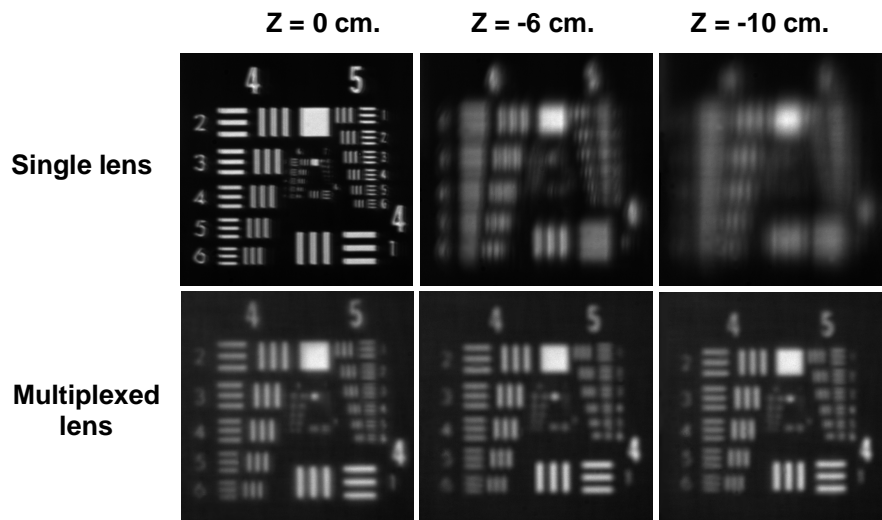


Fig. 12. Images of the resolution target captured at the best image plane ( $Z = 0$ ) and defocused planes ( $Z = -6$  cm and  $Z = -10$  cm) when a single lens and a multiplexed lens (M33) are used.

Images of the resolution target are shown in Fig. 12. They were captured in the same conditions as those corresponding to Fig. 11. It is clear that the M33 lens produces at  $Z = 0$  cm lower contrast and there is some decrease in resolution compared with the single lens. Nevertheless, the tests are still focused at the planes  $Z = -6$  cm and  $Z = -10$  cm with the M33 lens. On the contrary, they appear blurred for the single lens in that defocused planes. It is interesting to remark, that the image of the resolution test for the M33 lens is very similar at the three planes. That means that the image quality (resolution, etc.) along the extended focal depth is maintained.

#### 4. Conclusions

In this work we propose a combination of several diffractive lenses written onto a single programmable LCD to produce high focal depth. The lenses are spatially multiplexed in a random scheme onto the LCD. We choose an arbitrary focal range of 20 cm that is much wider than of the single lens (SL). Then, we study multiplexed lenses with different number of lenses to produce a good axial response. We show that the SL (single lens) produces a FWHM (full width at half maximum) of 1 cm, and the best multiplexed lens (M33) produces a FWHM of about 20 cm.

To analyze the quality of the image, different studies have been done. First, we compare the MTF of the single lens with that produced with the multiplexed lenses. In our case the multiplexing of 33 lenses (M33 lens) produces the best MTF in the defocused planes in comparison with the other multiplexed lenses. This MTF presents neither contrast inversions nor zero MTF values. Secondly, we have measured the PSF in different defocused planes to choose the multiplexed lens that produces the most constant PSF in the focal range. These experimental results show that in our case the M33 is the best solution. Thirdly, we compare experimental results with extended objects for the single lens and the M33 lens. These experimental results confirm that using this multiplexed lens the image quality with extended objects is very good in the defocused planes along the focal range.

#### Acknowledgments

We acknowledge financial support from the Spanish Ministerio de Ciencia y Tecnología (grant BFM2003-06273-C02-01/FISI) and from Generalitat de Catalunya (grant ACI2003-42). C. Iemmi gratefully acknowledges the support of the Universidad de Buenos Aires and Consejo Nacional de Investigaciones Científicas y Técnicas (Argentina).